

Article

Gas-Phase Fragmentation Reactions of Protonated Cystine using High-Resolution Tandem Mass Spectrometry

Pengwei Zhang ¹, Wan Chan ², Irene L. Ang ¹, Rui Wei ¹, Melody M. T. Lam ³, Kate M. K. Lei ¹ and Terence C. W. Poon ^{1,*}

¹ Pilot Laboratory, Institute of Translational Medicine, Faculty of Health Sciences, University of Macau, Macau, China; yb47620@connect.um.edu.mo (P.Z.); ireneang@um.edu.mo (I.L.A.); yb47623@connect.um.edu.mo (R.W.); katelei@um.edu.mo (K.M.K.L.)

² Department of Chemistry, Hong Kong University of Science and Technology, Hong Kong, China; chanwan@ust.hk

³ Proteomics Core, Faculty of Health Sciences, University of Macau, Macau, China; mantinglam@um.edu.mo

* Correspondence: tcwpoon@um.edu.mo; Tel.: +853-8822-4501

Received: 19 January 2019; Accepted: 14 February 2019; Published: 19 February 2019



Abstract: Cystine is an important biomolecule in living systems. Although collision-induced dissociation (CID)-based tandem mass spectrometry (MS/MS) is commonly applied for identification and quantification of cystine in both biomedical and nutritional studies, gas-phase fragmentation reactions of cystine in CID has remained unclear. This may lead to improper assay design, which may in turn result in inaccurate test results. In the present study, gas-phase fragmentation reactions of protonated cystine in CID were characterized using high-resolution MS/MS and pseudo MS³. Fragmentations started from cleavages of disulfide bond (S–S) and carbon–sulfur bond (C–S). When cleaving at the S–S, protonated cystine was generated as one of the predominant fragmentation products. Minor fragmentations started from the loss of H₂O + CO and the loss of NH₃. Our results reveal that the *m/z* 74 fragment ion, which is commonly used as a product ion of the transition (precursor/product ion pair) in selected reaction monitoring (SRM) assay for quantifying cystine, comprises two isobaric fragments originating from different parts of cystine. This indicates the need for careful selection of a stable isotope-labeled cystine molecule as an internal standard for SRM assays. Here, we provide a clear picture of the fragmentation reactions of protonated cystine in CID. It can serve as a useful guidance for designing MS/MS-based assays for cystine testing.

Keywords: cystine; cysteine; gas-phase fragmentation reaction; high-resolution MS/MS; pseudo MS³; isobaric fragment

1. Introduction

Studies of gas-phase fragmentation reactions of protonated amino acids, particularly in collision-induced fragmentation (CID), are crucial not only for their identification and quantification but also for facilitating the understanding of the fragmentation reactions of its analogous and small peptides [1–4]. Cystine, an oxidized form of cysteine, is a special dimer of cysteine. Although it is a nonproteinogenic amino acid, cystine plays important roles in a variety of cellular functions and is involved in metabolism pathways [5]. Cystine in urine, blood, or other biological samples has been used as an important biomarker for various pathological conditions, such as inherited metabolic disorders and cystinosis [4–6]. Quantification of cystine in leukocytes and urine by CID-based LC–MS/MS is performed in the clinical routine for diagnosis of nephropathic cystinosis [7–10]. Selected reaction monitoring (SRM) is the mostly reported method for measuring cystine [6–13].

Thus, a good knowledge of the gas-phase fragmentation chemistry of cystine in CID is essential to design MS/MS-based assays for reliable cystine testing. Furthermore, it can help in understanding the fragmentation chemistry of S–S and C–S bond-containing molecules, such as peptides and other biomolecules, which in turn facilitates development of strategies for structure elucidation [14].

To the best of our knowledge, MS/MS fragmentation reactions of protonated cystine in CID have only been reported by three research teams [4,14–16]. In total, nine fragment ions were reported at m/z 74, m/z 120, m/z 122, m/z 152, m/z 154, m/z 178, m/z 195, m/z 223, and m/z 224. Only two fragment ions at m/z 122 and m/z 195 were reported by all three research teams. The inconsistency could be due to the use of standard or in-house optimized MS/MS procedures in the three studies. Except the fragment ion at m/z 74, chemical identities were assigned to those observed fragmentation products [14–16]. It is important to note that, in all these experiments, their CID-based MS/MS platforms only had unit mass resolution, which could not resolve intramolecular isobaric fragment ions. This might have resulted in incorrect assignments of the chemical identities for the observed fragmentation products. Such annotation ambiguity can only be solved using high-resolution tandem mass spectrometry (HR-MS/MS) [17,18].

Because only limited information about the fragmentation chemistry of protonated cystine is available, the present study aimed to characterize the gas-phase fragmentation reactions of protonated cystine in CID using HR-MS/MS. Together with pseudo MS³ experiments, fragmentation reactions of the protonated cystine was clearly elucidated.

2. Results and Discussion

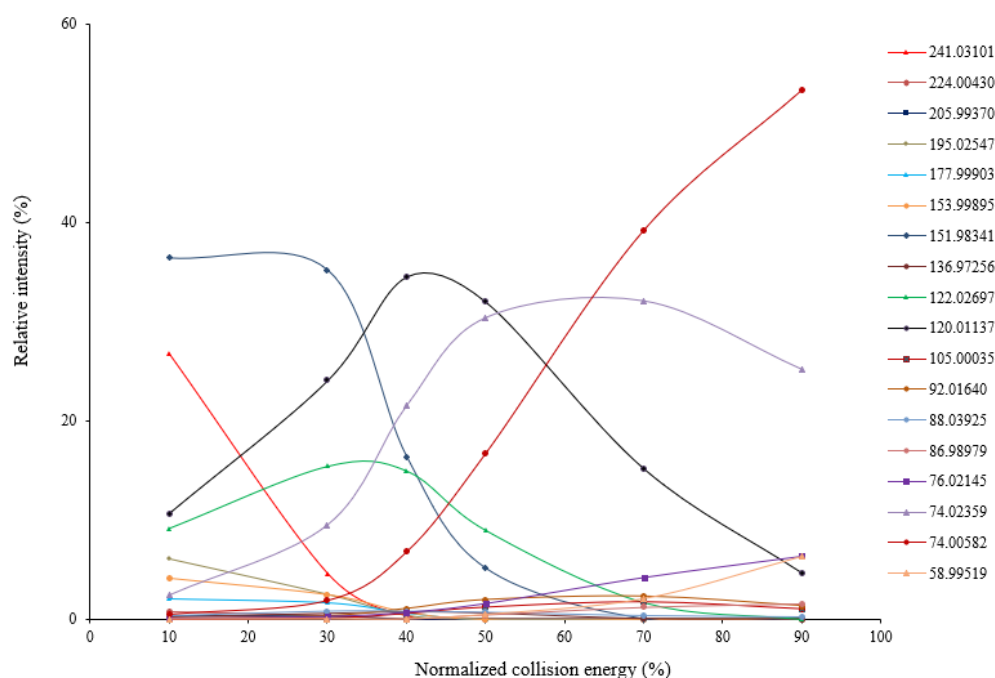
Using HR-MSMS operated at various levels of collision energy, gas-phase fragmentation of protonated cystine ($n = 3$) generated 17 reproducible fragment ions for which chemical identities were successfully assigned with a mass tolerance of 5 ppm. Sixteen of the 17 fragment ions had a mass error ≤ 1.5 ppm. Nine of the 17 fragment ions were observed in the previous studies using CID or other fragmentation techniques [4,14–16,19,20]. Their assigned chemical identities are summarized in Table 1. Under low collision energy (normalized collision energy, NCE $\leq 30\%$), the fragment ions at m/z 151.98341, m/z 122.02697, and m/z 120.01137 were the predominant fragmentation products (Figure 1). When the collision energy increased, their relative intensities decreased rapidly, and two isobaric fragment ions at m/z 74.02359 and 74.00582 became predominant. Using electron-induced dissociation (EID)-based HR-MS/MS, only the isobaric fragment ion at m/z 74.0240 was observed [16]. Relative intensities of other fragment ions were always low, regardless of the collision energy levels. Energy-resolved fragmentation graph of protonated cystine is provided in Figure 1.

MS/MS fragmentation reactions of protonated cystine mainly involved four major pathways with initial cleavages at the C–S bond and S–S bond (Figure 2a). First, a pair of fragment ions at m/z 151.98341 (loss of C₃H₇NO₂, major form) and m/z 153.99895 (loss of C₃H₅NO₂, minor form) was formed through the cleavage of C–S bond. The m/z 151.98341 fragment ion was fragmented to form the m/z 74.02359 fragment ion after the further loss of CH₂S₂ through the cleavage of C2–C3 or C2'–C3' bond. This fragmentation reaction was confirmed by pseudo MS³ analysis of the fragment ion at m/z 151.98341 (Figure 3a). Second, the cleavage of S–S bond generated two fragment ions at m/z 120.01137 and m/z 122.02697 by the loss of C₃H₇NO₂S and loss of C₃H₅NO₂S, respectively (Figure 2a). The m/z 120.01137 fragment ion was further dissociated to form two fragment ions at m/z 92.01640 and m/z 74.00582 by the loss of CO (Figure 2b) and loss of H₂O + CO (Figure 2b), respectively. These two fragments were also confirmed by pseudo MS³ analysis of the fragment ion at m/z 120.01137 (Figure 3b).

Table 1. Summary of m/z values and assigned chemical identities of fragmentation products of protonated cystine.

Protonated Cystine (Theoretical m/z)	Observed m/z Values of Fragment Ions ($n = 3$) ^a		Proposed Chemical Identity	Theoretical m/z	Mass Error (ppm)	Reported in Previous Studies [Reference] ^c
	Mean	SEM				
Cystine (241.03113)	224.00430	0.00007	$[M + H - NH_3]^+$	224.00458	-1.2	CID [4,15,16], others [19]
	205.99370	0.00015	$[M + H - NH_3 - H_2O]^+$	205.99401	-1.5	unreported
	195.02547	0.00006	$[M + H - H_2O - CO]^+$	195.02565	-0.9	CID [4,14-16]
	177.99903	0.00006	$[M + H - H_2O - CO - NH_3]^+$	177.99910	-0.4	CID [4,14-16]
	153.99895	0.00007	$[M + H - C_3H_5NO_2]^+$	153.99910	-1.0	CID [4,15,16]
	151.98341	0.00005	$[M + H - C_3H_7NO_2]^+$	151.98345	-0.2	CID [4,15,16], others [16,20]
	136.97256	0.00006	$[M + H - C_3H_5NO_2 - NH_3]^+$	136.97255	0.1	Unreported
	122.02697	0.00006	$[M + H - C_3H_5NO_2S]^+$	122.02703	-0.5	CID [4,14-16], others [16,20]
	120.01137	0.00006	$[M + H - C_3H_7NO_2S]^+$	120.01138	-0.1	CID [4,15,16], others [16,20]
	105.00035	0.00006	$[M + H - C_3H_5NO_2S - NH_3]^+$	105.00048	-1.3	unreported
	92.01640	0.00005	$[M + H - C_3H_7NO_2S - CO]^+$	92.01646	-0.7	unreported
	88.03925	0.00004	$[M + H - C_3H_5NO_2S - H_2S]^+$	88.03930	-0.6	others [16,20]
	86.98979	0.00005	$[M + H - C_3H_5NO_2S - NH_3 - H_2O]^+$	86.98989	-1.4	unreported
	76.02145	0.00003	$[M + H - C_3H_5NO_2S - H_2O - CO]^+$	76.02155	-1.3	unreported
	74.02359 ^b	0.00003	$[M + H - C_3H_7NO_2 - CH_2S_2]^+$	74.02365	-0.9	CID [4], others [16,20]
	74.00582	0.00003	$[M + H - C_3H_7NO_2S - H_2O - CO]^+$	74.00590	-1.1	unreported
	58.99519	0.00002	$[M + H - C_3H_5NO_2S - NH_3 - H_2O - CO]^+$	58.99500	3.2	unreported

^a The mean and standard error of mean (SEM) of the m/z values were calculated using the data from three independent experiments performed on different days. ^b Isobaric fragment ions are shown in bold. ^c Collision-induced dissociation (CID): fragmentation products generated by CID (unit mass resolution) [4,14-16]; others: fragmentation products generated by other fragmentation techniques, including electron-induced dissociation (high resolution) [16], field desorption (unit mass resolution) [19], and laser microprobe (unit mass resolution) [20]; unreported: fragmentation products not reported in any previous studies.

**Figure 1.** Energy-resolved fragmentation graph of protonated cystine under different collision energies.

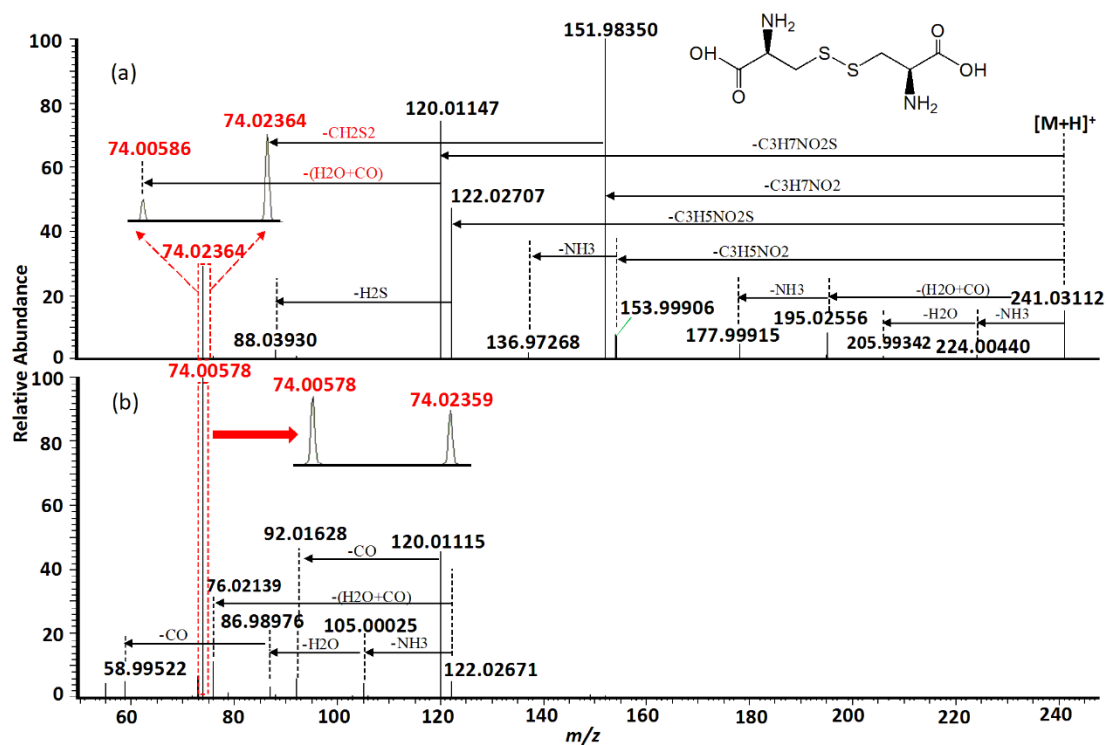


Figure 2. Representative MS/MS spectra of protonated cystine acquired using normalized collision energy (NCE) of (a) 30% and (b) 70%. Isobaric fragmentations are shown in red.

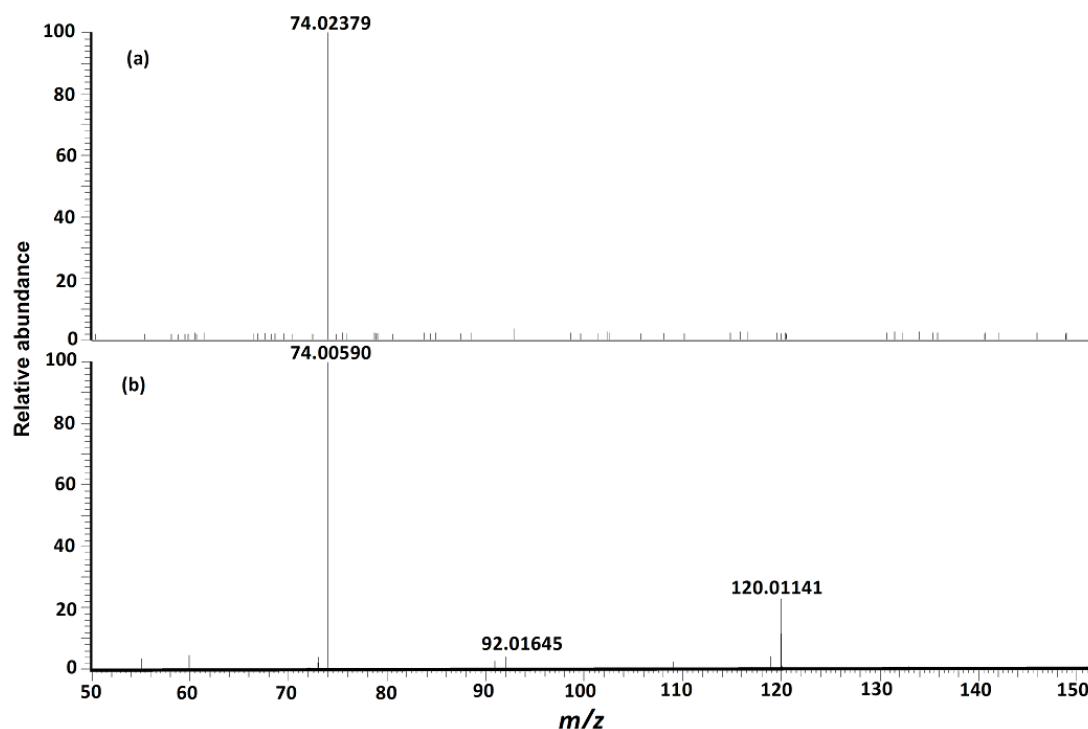


Figure 3. (a) Pseudo MS³ spectrum of fragment ion at m/z 151.98341 from protonated cystine, which supports the proposed fragmentation pathway for formation of fragment at m/z 74.02359. (b) Pseudo MS³ spectrum of the fragment ion at m/z 120.01137 from protonated cystine, which supports the proposed fragmentation pathway for formation of fragments at m/z 74.00582 and m/z 92.01640.

With respect to the loss of $C_3H_5NO_2S$, the m/z 122.02697 fragment should be protonated cysteine. This chemical identity was verified by examining its fragmentation products. Under low collision energy, the m/z 122.02697 fragment ion was dissociated to form a fragment ion at m/z 88.03925 with the loss of H_2S . Under high collision energy, the m/z 122.02697 fragment ion was dissociated to form a fragment ion at m/z 76.01245 after the loss of $H_2O + CO$, whereas sequential losses of NH_3 , H_2O , and CO from the m/z 122.02697 fragment ion led to the formation of fragment ions at m/z 105.00035, m/z 86.98979, and m/z 58.99519, respectively (Figure 2b). Except for the minor fragment ion at m/z 88.03925, all fragmentation products of the m/z 122.02697 fragment ion were identical with the previously reported MS/MS fragmentation products of protonated cysteine [21].

Besides the four major fragmentation pathways, there were two minor pathways for protonated cystine. Under low collision energy, the loss of $H_2O + CO$ and loss of NH_3 from protonated cystine resulted in the formation of two fragment ions at m/z 195.02547 and m/z 224.00430, respectively (Figure 2a), which is similar to the fragmentation of protonated α -amino acids [21]. A further loss of NH_3 from the m/z 195.02547 fragment led to the formation of a fragment ion at m/z 177.99903 (Figure 2a). The postulated fragmentation pathways of protonated cystine are presented in Figure 4.

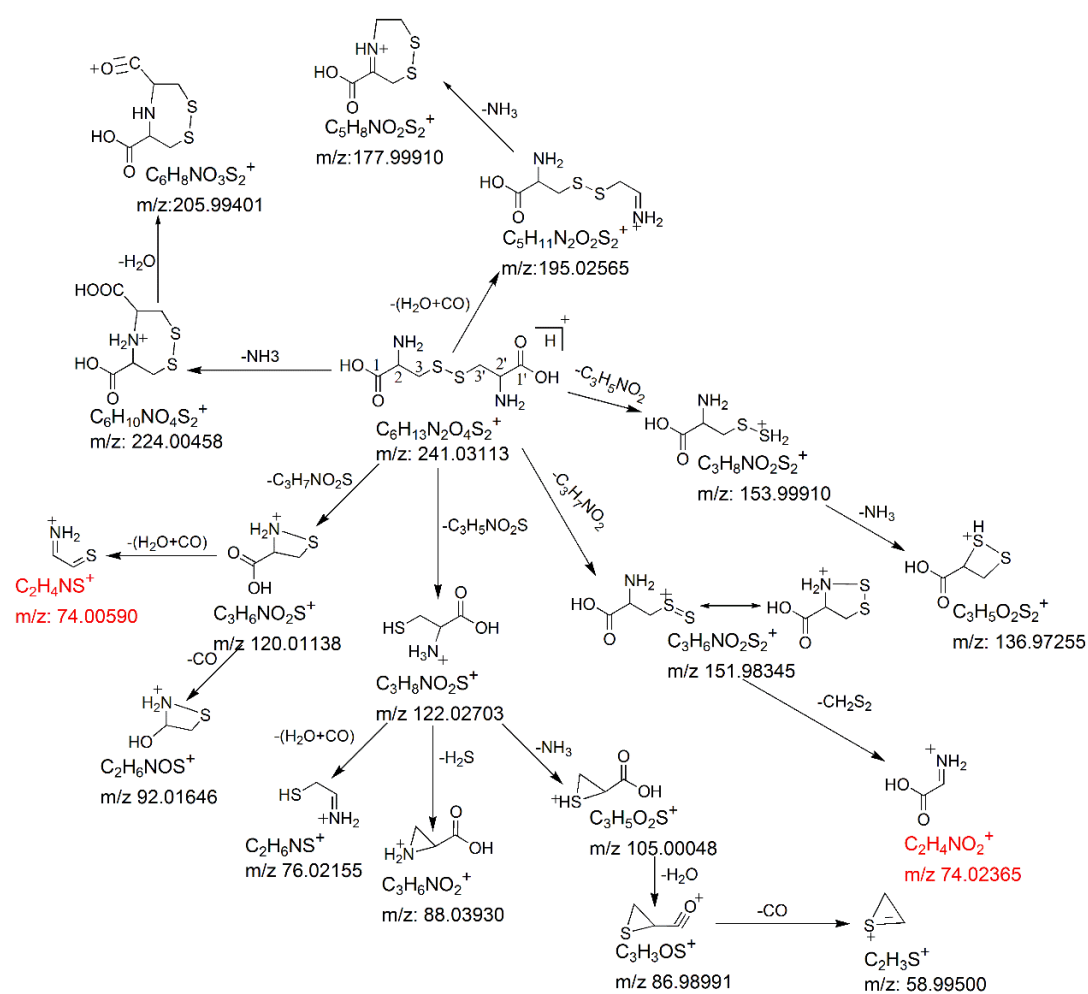


Figure 4. Postulated fragmentation pathways for protonated cystine in CID. The isobaric fragments are shown in red. The m/z values shown are the theoretical masses obtained by calculation.

Cystine plays an important role in biological systems. Its levels in biological samples are commonly measured by SRM. The SRM transition $241 \rightarrow 74$ [4,10,12,13,22] or $241 \rightarrow 152$ [6–9,11,22] is mostly used for cystine quantification to increase sensitivity. Our data showed that the m/z 152 fragment ion was predominant when the collision energy was low (Figure 2a). In contrast, the m/z 74

fragment ion was predominant when the collision energy was high (Figure 2b). Therefore, the selection between these two fragment ions as the product ion of the SRM transition for maximum sensitivity depended on the collision energy chosen in the SRM assay. Moreover, our data showed that the m/z 74 fragment ion comprised two isobaric fragments (i.e., theoretical monoisotopic masses of m/z 74.00590 and m/z 74.02365), which were originated from different parts of cystine (Figure 4) and had similar intensities (Figure 2b). The m/z 74.00590 fragment ion contained carbon atoms at the C2 and C3 positions or at the C2' and C3' positions, whereas the m/z 74.02365 fragment ion contained carbon atoms at the C1 and C2 positions or at the C1' and C2' positions. In SRM assays, stable isotope-labeled cystine is spiked into the samples and used as an internal standard. Some examples of commercially available stable isotope-labeled cystine are cystine-1,1'- $^{13}\text{C}2$ (Example 1), cystine- $^{15}\text{N}2$ (Example 2), cystine-3,3,3',3'-d4 (Example 3) and cystine- $^{15}\text{N}2$ -1,2,3,1',2',3'- $^{13}\text{C}6$ (Example 4). Corresponding to the pair of m/z 74 isobaric fragment ions (i.e., m/z 74.00590 and m/z 74.02365) from unlabeled cystine, Example 1 will generate two fragment ions at m/z 74 and m/z 75; Example 2 will generate two fragment ions at m/z 75 and m/z 75; Example 3 will generate two fragment ions at m/z 76 and m/z 74; and Example 4 will generate two fragment ions at m/z 78 and m/z 78. Only Example 2 and Example 4 will generate two isobaric fragment ions, whereas Example 1 and Example 3 will generate two fragment ions of different masses. In Example 1 and Example 3, one of the fragment ions is exactly the same as the corresponding m/z 74 fragment ion from unlabeled cystine. If Example 1 or Example 3 is selected as an internal standard in a SRM assay that uses transition 241 \rightarrow 74 for measuring signal intensity from endogenous cystine (unlabeled) in a sample, the m/z 74 fragment ion from the internal standard will interfere the signal intensity of the m/z 74 fragment ion from the endogenous cystine. These simple examples indicate the importance of careful selection of a stable isotope-labeled cystine molecule as an internal standard for SRM assays.

In conclusion, gas-phase fragmentation reactions of protonated cystine in CID were characterized using HR-MS/MS for the first time. Here, we provide a clear picture of the fragmentation reactions of protonated cystine in CID. This can serve as a useful guidance for designing MS/MS-based assays for cystine testing.

3. Materials and Methods

3.1. Materials

L-cystine (purity = 99.9%, pharmaceutical secondary standard, Cat. No. PHR1323, Lot. No. LRAA0826) was obtained from Sigma-Aldrich, St. Louis, MO, USA. LC-MS grade formic acid (FA), water and acetonitrile (ACN) were obtained from Thermo Fisher Scientific, Pierce Chemical, Rockford, IL, USA. L-Cystine stock solution was prepared in MS grade water containing 0.1 M HCl and stored at -80 °C. Before analysis, the stock solution was diluted to 5 μM working solution using ACN/water (1:1).

3.2. High-Resolution Tandem Mass Spectrometry (HR-MS/MS)

MS/MS fragmentations by HCD, which is a CID technique specific to the orbitrap mass spectrometer, were conducted on a Q Exactive Hybrid Quadrupole-Orbitrap Mass Spectrometer (Thermo Fisher Scientific, Waltham, MA, USA) equipped with a heated electrospray source. The MS/MS parameters were set as follows: MS/MS resolution, 70,000; automatic gain control (AGC), 5×10^5 ; injection time, 250 ms; isolation window, 0.4 Da. Ten microliters quantity of the working solution was directly injected to the MS by a UHPLC (UltiMate 3000 RSLCnano System, Thermo Fisher Scientific, Waltham, MA, USA) with an autosampler using an isocratic gradient of 50% ACN containing 0.1% FA at a flow rate of 0.1 mL/min. The ion source parameters were set as follows: spray voltage, 3.0 kV; sheath gas, 25 (arbitrary unit); Aux gas, off; Aux gas heat, off. For pseudo MS³ acquisition, an in-source fragment from the parent ion was isolated by the quadrupole (size of isolation window = 0.4 Da) and fragmented in the collision cell. The experiments were conducted in triplicates on different days. Data obtained from the triplicate experiments were used to calculate the mean

values of the relative intensity (relative to the total fragment intensity) and m/z value of each fragment. Chemical identities were assigned to the fragment ions with mass tolerance of 5 ppm.

Author Contributions: P.Z. performed MS/MS analysis, pseudo MS³ with contributions from R.W., M.M.T.L., and K.M.K.L.; P.Z. performed data interpretation, data organization, and manuscript writing under the guidance of W.C., I.L.A and T.C.W.P.; T.C.W.P. conceived the study.

Funding: This research was funded by the Multi-Year Research Grant (MYRG) of University of Macau (RC Reference Number: MYRG2015-00233-FHS).

Conflicts of Interest: The authors declare no conflict of interest.

References

1. Talaty, E.R.; Young, S.M.; Dain, R.P.; Van Stipdonk, M.J. A study of fragmentation of protonated amides of some acylated amino acids by tandem mass spectrometry: Observation of an unusual nitrilium ion. *Rapid Commun. Mass Spectrom.* **2011**, *25*, 1119–1129. [[CrossRef](#)] [[PubMed](#)]
2. Guan, X.; Wang, B.; Wang, H.; Liu, J.; Li, Y.; Guo, X. Characteristic NH₃ and CO losses from sodiated peptides C-terminated by glutamine residues. *Rapid Commun. Mass Spectrom.* **2017**, *31*, 649–657. [[CrossRef](#)] [[PubMed](#)]
3. Kotiaho, T.; Eberlin, M.N.; Vainiotalo, P.; Kostianen, R. Electrospray mass and tandem mass spectrometry identification of ozone oxidation products of amino acids and small peptides. *J. Am. Soc. Mass Spectrom.* **2000**, *11*, 526–535. [[CrossRef](#)]
4. Piraud, M.; Vianey-Saban, C.; Petritis, K.; Elfakir, C.; Steghens, J.-P.; Morla, A.; Bouchu, D. ESI-MS/MS analysis of underivatized amino acids: A new tool for the diagnosis of inherited disorders of amino acid metabolism. Fragmentation study of 79 molecules of biological interest in positive and negative ionisation mode. *Rapid Commun. Mass Spectrom.* **2003**, *17*, 1297–1311. [[CrossRef](#)] [[PubMed](#)]
5. Yu, X.; Long, Y.C. Crosstalk between cystine and glutathione is critical for the regulation of amino acid signaling pathways and ferroptosis. *Sci. Rep.* **2016**, *6*, 30033. [[CrossRef](#)] [[PubMed](#)]
6. Johnson, J.M.; Strobel, F.H.; Reed, M.; Pohl, J.; Jones, D.P. A rapid LC-FTMS method for analysis of cysteine, cystine and cysteine/cystine steady-state redox potential in human plasma. *Clin. Chim. Acta* **2008**, *396*, 43–48. [[CrossRef](#)] [[PubMed](#)]
7. Wear, J.E.; Keevil, B.G. Measurement of Cystine in Urine by Liquid Chromatography–Tandem Mass Spectrometry. *Clin. Chem.* **2005**, *51*, 787–789. [[CrossRef](#)]
8. Bose, N.; Zee, T.; Kapahi, P.; Stoller, M.L. Mass Spectrometry-based in vitro Assay to Identify Drugs that Influence Cystine Solubility. *Bio-protocol* **2017**, *7*, e2417. [[CrossRef](#)]
9. Jamalpoor, A.; Sparidans, R.W.; Pou Casellas, C.; Rood, J.J.M.; Joshi, M.; Masereeuw, R.; Janssen, M.J. Quantification of cystine in human renal proximal tubule cells using liquid chromatography-tandem mass spectrometry. *Biomed. Chromatogr.* **2018**, *32*, e4238. [[CrossRef](#)]
10. Piraud, M.; Vianey-Saban, C.; Bourdin, C.; Acquaviva-Bourdain, C.; Boyer, S.; Elfakir, C.; Bouchu, D. A new reversed-phase liquid chromatographic/tandem mass spectrometric method for analysis of underivatized amino acids: Evaluation for the diagnosis and the management of inherited disorders of amino acid metabolism. *Rapid Commun. Mass Spectrom.* **2005**, *19*, 3287–3297. [[CrossRef](#)]
11. Zee, T.; Bose, N.; Zee, J.; Beck, J.N.; Yang, S.; Parihar, J.; Yang, M.; Damodar, S.; Hall, D.; O’Leary, M.N.; et al. α -Lipoic acid treatment prevents cystine urolithiasis in a mouse model of cystinuria. *Nat. Med.* **2017**, *23*, 288–290. [[CrossRef](#)] [[PubMed](#)]
12. Kang, Y.P.; Torrente, L.; Liu, M.; Asara, J.M.; Dibble, C.C.; DeNicola, G.M. Cysteine dioxygenase 1 is a metabolic liability for non-small cell lung cancer. *bioRxiv* **2018**, 459602. [[CrossRef](#)]
13. Choi, M.S.; Rehman, S.U.; Kim, I.S.; Park, H.-J.; Song, M.-Y.; Yoo, H.H. Development of a mixed-mode chromatography with tandem mass spectrometry method for the quantitative analysis of 23 underivatized amino acids in human serum. *J. Pharm. Biomed. Anal.* **2017**, *145*, 52–58. [[CrossRef](#)] [[PubMed](#)]
14. Butler, M.; Siu, K.M.; Hopkinson, A.C. Transnitrosylation products of the dipeptide cysteinyl-cysteine: An examination by tandem mass spectrometry and density functional theory. *Phys. Chem. Chem. Phys.* **2016**, *18*, 6047–6052. [[CrossRef](#)] [[PubMed](#)]

15. Lioe, H.; O'Hair, R.A.J. A novel salt bridge mechanism highlights the need for nonmobile proton conditions to promote disulfide bond cleavage in protonated peptides under low-energy collisional activation. *J. Am. Soc. Mass Spectrom.* **2007**, *18*, 1109–1123. [[CrossRef](#)] [[PubMed](#)]
16. Lioe, H.; O'Hair, R.A.J. Comparison of collision-induced dissociation and electron-induced dissociation of singly protonated aromatic amino acids, cystine and related simple peptides using a hybrid linear ion trap-FT-ICR mass spectrometer. *Anal. Bioanal. Chem.* **2007**, *389*, 1429–1437. [[CrossRef](#)] [[PubMed](#)]
17. Clemen, M.; Gernert, C.; Peters, J.; Grottemeyer, J. Fragmentation reactions of labeled and unlabeled Rhodamine B in a high-resolution Fourier transform ion cyclotron resonance mass spectrometer. *Eur. J. Mass Spectrom.* **2013**, *19*, 135–139. [[CrossRef](#)]
18. Thurman, E.M.; Ferrer, I.; Benotti, M.; Heine, C.E. Intramolecular Isobaric Fragmentation: A Curiosity of Accurate Mass Analysis of Sulfadimethoxine in Pond Water. *Anal. Chem.* **2004**, *76*, 1228–1235. [[CrossRef](#)]
19. Winkler, H.U.; Beckey, H.D. Field desorption mass spectrometry of amino acids. *Org. Mass Spectrom.* **1972**, *6*, 655–660. [[CrossRef](#)]
20. Verbueken, A.H.; Van Grieken, R.E.; De Broe, M.E.; Wedeen, R.P. Identification of inorganic and organic microliths in kidney sections by laser microprobe mass spectrometry. *Anal. Chim. Acta* **1987**, *195*, 97–115. [[CrossRef](#)]
21. Dookeran, N.N.; Yalcin, T.; Harrison, A.G. Fragmentation Reactions of Protonated α -Amino Acids. *J. Mass Spectrom.* **1996**, *31*, 500–508. [[CrossRef](#)]
22. McGaw, E.A.; Phinney, K.W.; Lowenthal, M.S. Comparison of orthogonal liquid and gas chromatography-mass spectrometry platforms for the determination of amino acid concentrations in human plasma. *J. Chromatogr. A* **2010**, *1217*, 5822–5831. [[CrossRef](#)] [[PubMed](#)]

Sample Availability: Samples of the compounds are not available from the authors.



© 2019 by the authors. Licensee MDPI, Basel, Switzerland. This article is an open access article distributed under the terms and conditions of the Creative Commons Attribution (CC BY) license (<http://creativecommons.org/licenses/by/4.0/>).